BIO-REFINERY APPROACH FOR THE CONVERSION OF BIOMASS WASTE INTO RENEWABLE POLYMER AND BIOETHANOL AS A FUEL ADDITIVE

Mohammed A. Asmer, Ahmed G. S. Al-Azzawi*

Chemistry department, Education College for Pure Science, University of Mosul
**e-mail: amsss82@uomosul.edu.iq*

Received 13.03.2026
Accepted 08.06.2026

Abstract: *In this current study, cotton stalks were utilized as a sustainable lignocellulosic feedstock for the integrated production of cellulose acetate and bioethanol. In the initial step, cellulose extracted from biomass was chemically modified into cellulose acetate via an acetylation process. The successful conversion and physicochemical properties of the obtained cellulose acetate were confirmed using multi-analysis techniques, including Nuclear Magnetic Resonance (NMR) spectroscopy, Gel Permeation Chromatography (GPC) analysis, elemental composition (CHNS) analysis, Thermogravimetric analysis (TGA), X-ray diffraction (XRD) test, and Scanning Electron Microscopy (SEM). The obtained results indicated an effective acetylation process of cellulose, leading to structural changes in morphological surface, crystallinity, thermal stability, and functional groups over polymer chains. In the second stage, the biomass feedstock was subjected to mechanical and chemical pretreatment using phosphoric acid (H_3PO_4) at concentrations of 0.5%, 1.0%, and 1.5% to facilitate the lignocellulosic hydrolysis and enhance fermentable sugar yields in the broth. The pretreated biomass was fermented using S. cerevisiae under controlled conditions (32℃, pH=4-5, 72 hours), producing bioethanol yields of 20.1%, 37.5%, and 34.5%, respectively. It can be noted that the highest yield of obtained bioethanol at 1% acid concentration is ascribed to optimal lignocellulosic structure disruption, which improves cellulose accessibility and fermentable sugar levels, whereas higher acid concentrations may lead to partial sugar degradation and the formation of inhibitors that limit the efficiency of the fermentation performance. The obtained bioethanol was mixed with pure gasoline at 5%, 7%, and 10% (v/v) to assess its performance as a sustainable fuel additive. The fuel binary mixtures exhibited an increase in RON values compared to the normal gasoline. This is mainly attributed to the oxygenated nature and antiknock behavior of bioethanol. Moreover, fuel density and RVP values remained within acceptable gasoline specifications, confirming the suitability of these fuel blends for conventional internal combustion engines. Overall, this study highlighted the promising approach for transforming biomass into valuable cellulose derivatives and sustainable bioethanol, enhancing sustainable biomass utilization and clean energy production.*
Keywords*: Cotton stalks, Acetylation reaction, Bioconversion process, Bioethanol, Fuel binary mixtures.*

1. Introduction

Agricultural residues represent vast, largely untapped resources for the sustainable production of high-value materials and renewable fuels [1, 2]. Among these residues, cotton stalks (the lignocellulosic biomass left after cotton) are harvested, which are produced globally in quantities exceeding millions of tons annually, yet are predominantly employed in low-value approaches, such as low-grade energy application, such as direct burning [3-5]. Cotton stalks consist mainly of cellulose, hemicellulose, and lignin, making them a viable feedstock for biochemical and chemical transformation routes [6]. Cellulose is considered the most abundant biopolymer on Earth, which has received considerable research attention due to its abundance, renewability, biodegradability, and versatile chemical functionality [7-10]. Among the industrial derivatives of cellulose, cellulose acetate (CA) is widely used as a biopolymer in films, coatings, fibers, and plastics due to its tunable favorable physicochemical properties [11, 12]. Traditional CA production requires highly purified cellulose sources. However, a previous study has focused on the acetylation of lignocellulosic biomass, including cotton stalks, as a main strategy to upgrade agricultural waste to cellulose acetate-based polymer [13, 14]. Cellulose isolated from pre-treated cotton stalks can be successfully converted to CA through acetylation using acetic acid and acetic anhydride under acidic conditions,

and optimization using response surface methodology, leading to high acetyl content and successful polymer formation, as revealed by FT-IR and XRD analysis [13, 15-17].

Recently, cotton stalks have been widely studied as a promising feedstock for bioethanol production owing to their high cellulose content. Following effective pretreatment to break down the lignin-hemicellulose matrix. Fermentable sugars can be produced from cellulose through enzymatic hydrolysis, which are subsequently converted into bioethanol via a microbial fermentation process [1, 2, 9]. This strategy offers a renewable alternative to fossil fuels and supports a global sustainable energy system to mitigate climate change, thereby reducing dependence on fossil fuels and avoiding competition with food resources by utilizing non-food biomass residues. Previous studies indicated that dilute acid and alkali pretreatment significantly increases the yield of accessible cellulose and subsequent sugar, which forms the basis of enzymatic hydrolysis and yeast fermentation to bioethanol [18, 19]. In addition, advanced fermentation approaches, such as co-fermentation with immobilized yeast, have been reported to enhance ethanol production from pretreated cotton stalk feedstock [20, 21]. The objective of this current work is to convert cotton stalks to beneficial products via an integrated bioconversion process.

2. Experimental part

Materials used. All reagents, chemicals, and solvents used were provided by commercial suppliers and utilized as received without further purification. While the feedstock material (cotton stalk) was locally collected from the Al-Hawija district, Kirkuk, Iraq.

Instrument section. The chemical structure, composition, properties, and purity of the resulting products were verified using different analytical techniques. NMR spectroscopy was performed using a Bruker (Avance NEO-X 400 MHz). FTIR spectroscopy was conducted on a Bruker (ALPHA II) spectrometer, recorded in the range of 400-4000 cm^{-1}. The molecular weight of the synthesized polymer was evaluated by GPC analysis using Azura (Knauer GPC/SEC lab system), calibrated with polystyrene standards, providing weight average-molecular weight (M_w), number average-molecular weight (M_n), and Polydispersity index (PDI). TGA measurements were carried out using a TA instrument (SDT Q600 V20.9 Build 20) to evaluate the thermal stability of materials under nitrogen conditions in the temperature range of ambient temperature to 1000 °C at a heating rate of 10 °C min^{-1}. The elemental composition (CHNS) of the obtained polymer was determined using the FlashSmart-CHNS/O analyzer (Eager 300 software). An XRD test was conducted on a Philips PW1730 (PANalytical Xpert high-score) X-ray diffractometer to investigate the crystallinity features of materials, operating with Cu Kα radiation (λ= 1.5 Å) over a 2θ range of 10-80° C. The morphological characteristics of the synthesized polymer were examined by SEM-Mira II Tescan at controlled accelerating voltages. The moisture content of pure gasoline and bioethanol-gasoline blend sample was evaluated using a digital coulometric titrator (Koehler AKF5000). The RON values of the base gasoline and its binary blends were determined using a Cooperative Fuel Research (CFR) engine equipped with a single-cylinder four-stroke spark ignition configuration. The RVP of the fuel samples was estimated using a digital RVP apparatus (Eralytics Eravap, Vapour Pressure Tester). Density measurements of the fuel blends were evaluated using a digital density meter (Rudolph Research Analytical density meter, DDM 2911).

Synthesis routes.

Collection and preparation of biomass samples. Cotton stalks were collected and then washed with distilled water to remove dust and adhering impurities, followed by air drying. The dried biomass was milled to obtain a yellow powder material, and then dried in an oven at 90 °C for 4 hours. The obtained powder was stored for further usage.

Isolation of cellulose from biomass.

Alkaline pretreatment of biomass. The method was designed according to a previous report by Silverstein [22]. The dried cotton stalk powder (40 g) was treated with the base solution (12.5% NaOH solution) at a solid-to-solution ratio of 1:10 (w/v). The resulting mixture was refluxed at 150-160 °C for 3 hours under stirring conditions to eliminate the hemicellulose component and partially

solubilize lignin from cotton stalk material. After the refluxing process, the suspension solution was cooled to ambient temperature, and then the solid fraction was separated by filtration and repeatedly washed with hot distilled water until the filtrate reached neutral pH (pH= 6-7). The solid residue (pulp) was collected and dried in an oven at 90 C for 3 hours to yield the brown solid product (13.8 g, 34.5%).

Bleaching of pulp. The synthesis procedure was adopted according to established literature by Wang [18]. The alkali-pretreated material (10 g) was subjected to a bleaching reaction using acidified sodium chlorite solution (5% $NaClO_2$), with the pH adjusted to 4-5 using acetic acid. The resulting mixture was heated up to reflux at 80 °C for 3 hours under stirring conditions. The resulting product was thoroughly washed with distilled water and dried at 80 C for 3 hours to yield white cellulose pulp as a pure product (7.28 g, 72.8%).

Synthesis of cellulose acetate. The synthetic approach was described by Heinze [23] and Edgar [24]. Purified cellulose (4 g) was suspended in 150 mL of acetic acid and stirred vigorously at normal temperature for 1 hour under inert conditions to allow cellulose swelling. Subsequently, a mixture of vinyl acetate (50 mL) and potassium carbonate (0.5 g) was added slowly to the suspension under stirring. The reaction mixture was heated to 60°C for 24 hours. After completion, the mixture was cooled to ambient temperature and then precipitated from a solution of cold methanol to water (8:2) to yield a white fiber. The obtained product was filtered and then washed with 50 mL of methanol (twice) and 50 mL of acetone (twice). The cellulose acetate product was dried in an oven at 60°C until constant weight to yield white fibers as a final product (3.6 g, 90%). ^{1}H-NMR (using deuterated dimethyl sulfoxide DMSO) (δ/ppm): 1.87-2.07 (m), 3.39-3.66 (m), 4.35 (s). ^{13}C NMR (δ/ppm): 20.67, 21.04, 169. GPC: (M_w =37.091 g/mol), (M_n =36.213 g/mol), (PDI =1.02). Elemental analysis (CHNS) for cellulose acetate: H, 5.88%; C, 40.65%; S, 0%; N, 0%; O, 53.47%.

Conversion of cotton stalk to bioethanol.

Acidic pretreatment and fermentation process of biomass. The method was performed following the modified procedure described by Alsaayigh [2]. The dried cotton stalk powder (200 g) was individually treated with dilute phosphoric acid solutions (0.5%, 1.0%, 1.5%) at a liquid-to-solid ratio of 10:1 (v/wt.). In a separate vessel (3 L), each mixture was refluxed in a flask equipped with a condenser for 3 hours to hydrolyze the biomass. Afterwards, the mixture was allowed to cool to normal temperature and then filtered using filter paper. Following pretreatment, neutralization was performed by repeatedly washing with distilled water until the pH reached 4-5. The suspension was filtered to obtain the solid material as a thick slurry. The resulting biomass was dried in an oven at 95 °C for 4 hours. It is worth mentioning that different acid concentrations with a constant acid-to-solid ratio were examined to determine the optimal conditions for bioethanol yield. The acid pretreated substrate was transferred into a sealed flask containing 4 L of distilled water to produce the fermentation broth. Following the hydrolysis step, the fermentation reaction was initiated using commercially available dry yeast (S. cerevisiae). After adjusting the pH to 4-5, an inoculum of activated yeast (20 g, 10% w/w) with pure urea (7 g, 3.5%) was added to the fermentation broth under inert continuous stirring. The mixture was incubated anaerobically at 32 °C for 72 hours to ensure maximum release of fermentable sugars to achieve optimal bioethanol production. Upon completion of the fermentation process, the broth was subjected to simple distillation between 78-80 °C to separate the crude bioethanol. The alcohol content was estimated using hydrometer analysis. Following completion, the resulting bioethanol was purified by fractional distillation at 78 ^{o}C, resulting in high-purity bioethanol (90-93%). Subsequently, the distillate was dehydrated using 3 Å molecular sieves to yield absolute bioethanol. The yield of alcohol was calculated according to the following equation:

$$\left\{\%\ Bioethanol = \frac{volume\ of\ bioethanol\ obtained\ (mL) \times\ ethanol\ density\ (0.789\ g/mL)}{weight\ of\ substrate\ (g)} \times 100\right\}$$

Furthermore, the purity and structure of the obtained bioethanol were verified through FTIR, ^{1}H and ^{13}C NMR spectroscopy.

^{1}H NMR (using deuterated chloroform $CHCl_3$) (δ/ppm): 0.91 (s), 3.47 (s), 4.62 (s). ^{13}C NMR (δ/ppm): 17.55, 57.08.

Gasoline blending and characteristics. In this study, a series of fuel formulations (E0, E5, E7, and E10) was prepared by mixing base gasoline with pure bioethanol at volumetric proportions of 0%, 5%, 7%, and 10% (v/v), respectively. Each binary mixture was prepared at a total volume of 500 mL using a laboratory shaker to ensure homogeneity. The physicochemical properties of the conventional gasoline and ethanol-gasoline blends were determined in accordance with ASTM standard methods, including density test (ASTM D4052) [25], Reid vapor pressure (RVP) test (ASTM-D6378) [26], Research octane number (RON) test (ASTM-D2699) [27], and moisture content test (ASTM method D6304) [28]. All tests on the fuel blends were performed using a range of standardized laboratory equipment [29].

3. Result and discussion

Synthesis of cellulose acetate. Cotton stalk feedstock is mainly composed of cellulose as the major component along with hemicellulose, lignin, extractives, and mineral ash. Isolation of the cellulose fraction requires a special treatment approach to eliminate non-cellulosic fractions without degrading the cellulose chains. In the pulping step as shown in Scheme 1, alkaline treatment with NaOH efficiently disrupts the structural integrity of the lignin-carbohydrate complex. Under alkaline conditions, the process facilitated the solubilization of lignin and hemicellulose fragments into the liquid phase as a result of cleavage of ester and ether linkages between lignin and hemicellulose. Furthermore, the alkaline medium improves fiber swelling by disrupting intermolecular hydrogen bonding, leading to an increase in the exposure of the internal hydroxyl groups. The alkaline pretreatment step yielded 34.5% solid residue, suggesting efficient elimination of lignin and hemicellulose fragments from the cotton stalk.

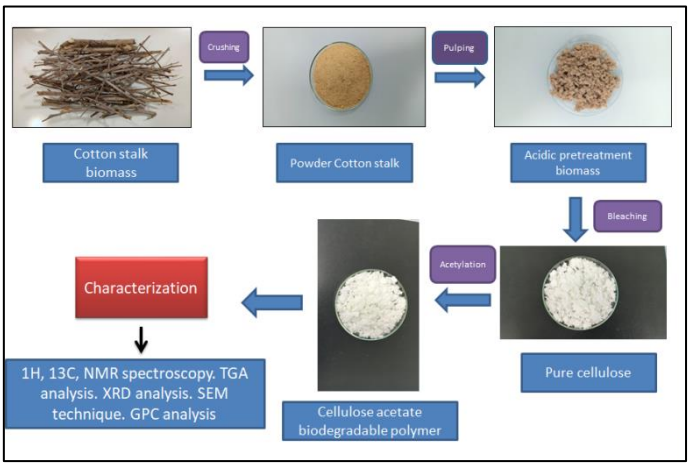

Scheme 1. Schematic diagram of cotton stalk and extraction process to obtain cellulose acetate.

The mass reduction can be attributed to the solubilization of non-cellulosic fractions, resulting in cellulose-rich fragments suitable for subsequent bleaching and acetylation steps. After alkaline

pretreatment, the pretreated biomass was subjected to a bleaching process using sodium chlorite to eliminate remaining lignin and trace hemicellulose fragments. This oxidative treatment disrupted aromatic lignin structures into soluble, low-molecular-weight derivatives. During the bleaching stage, phenolic lignin networks are converted into a soluble product, resulting in the degradation of chromophoric groups that are responsible for the dark coloration. This leads to an increase in cellulose crystallinity. It can be noticed that the final product (cellulose) was obtained as bright white crystals, indicating a high degree of cellulose purity. The visible color change from brown to bright white indicated a progressive bleaching process due to a significant reduction in lignin content.

The purified cellulose was effectively acetylated using vinyl acetate to produce cellulose acetate as a modified polymer. It can be observed that the formation of the esterified product was verified by its improved solubility in organic solvents such as DMSO and acetone, in contrast to the native form (pure cellulose). The high yield (90%) indicated the relatively high conversion of hydroxyl groups to esters under controlled reaction conditions. It is worth mentioning that the use of vinyl acetate as an acetylating agent and K_2CO_3 as a catalyst represents a more sustainable alternative to the conventional cellulose acetylation process based on acetic anhydride and sulfuric acid. Unlike strong acid catalysts, K_2CO_3 is mild, less corrosive, inexpensive, and reduces cellulose depolymerization. In addition, vinyl acetate enables acetylation through a transesterification mechanism that does not generate acidic by-products; the coproduct vinyl alcohol rapidly tautomerizes to volatile acetaldehyde, which is easily removed and shifts the reaction toward ester formation. Consequently, this approach minimizes acidic waste generation, lowers equipment corrosion, and helps preserve the molecular weight of cellulose while achieving efficient acetylation under relatively mild conditions. Polymer purity was evaluated through multiple analytical techniques, including NMR spectroscopy, GPC, and CHNS analysis. The GPC analysis of the synthesized cellulose acetate exhibited a moderate molecular weight with M_n=36.213 g.mol^{-1} and Mw=37.091 g.mol^{-1}, resulting in a PDI of 1.02. Such a low PDI value suggests a narrow molecular weight distribution, implying that the acetylation reaction occurred without significant degradation of the cellulose chains. In comparison with native cellulose, the measured molecular weight value of cellulose acetate indicates that the main polymer backbones were largely retained through the acetylation process. Overall, the obtained data confirmed the successful formation of cellulose acetate with a stable molecular structure, supporting its potential applications such as membranes, films, and biodegradable polymers.

Characterization of the synthesized cellulose acetate.

^{1}H and ^{13}C NMR analysis of cellulose acetate polymer. The conversion of cellulose to cellulose acetate was successfully verified using ^{1}H and ^{13}C NMR spectroscopy. The ^{1}H NMR spectrum (Fig. 1) exhibited distinct proton signals corresponding to the cellulose backbone and the attached acetyl groups.

The multiple peaks detected in the range of 1.87-2.08 ppm, corresponding to the methyl protons (-$COCH_3$) of the acetyl moieties, suggest the formation of cellulose ester linkage as clear evidence. The resonance multiple peaks between 3.3 and 5.0 ppm are assigned to the protons of an anhydroglucose backbone (H-2 to H-6). It can be noted that the anomeric proton (H-1) is located at 4.4-4.7 ppm, while other ring protons appear across 3.5-4.5 ppm. It is worth mentioning that the peaks at 2.50 and 3.39 ppm are attributed to residual DMSO solvent and trace water in the solvent, respectively. The observed spectral pattern agrees with previous studies of ^{1}H-NMR analysis of cellulose acetate in the literatures [23, 30]. The resulting data verified the successful acetylation of cellulose obtained from biomass.

Moreover, ^{13}C NMR analysis verified the transformation of cellulose into cellulose acetate, suggesting successful chemical modification. The recorded spectrum (Fig. 2) exhibited features consistent with the cellulose structure as well as the attached acetyl moieties. The peaks appeared at 20.6-21.0 ppm, corresponding to acetyl methyl carbon, which confirms the formation of an ester linkage. Additionally, another intense signal detected in the 39.2-40.5 ppm range is associated with the residual DMSO solvent carbon. It can be noted that weak peaks observed at 169-171 ppm are

attributed to the ester carbonyl carbon (C=O). The observed data are in good agreement with previous ^{13}C NMR reports on cellulose acetate [31, 32]. In summary, the ^{1}H and ^{13}C NMR spectra verified the formation of cellulose acetate and indicated that the acetylation process occurred without depolymerization of the cellulose backbone.

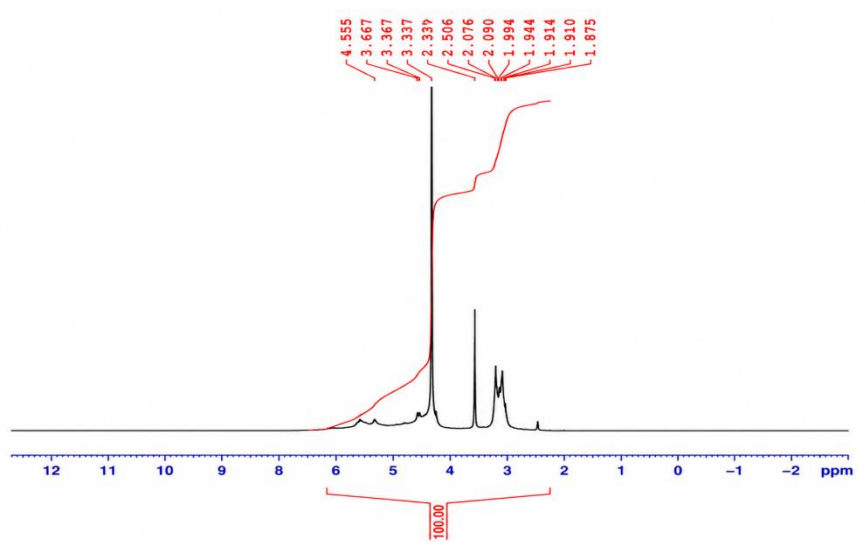

Fig. 1. ^{1}H NMR spectrum of the synthesized cellulose acetate

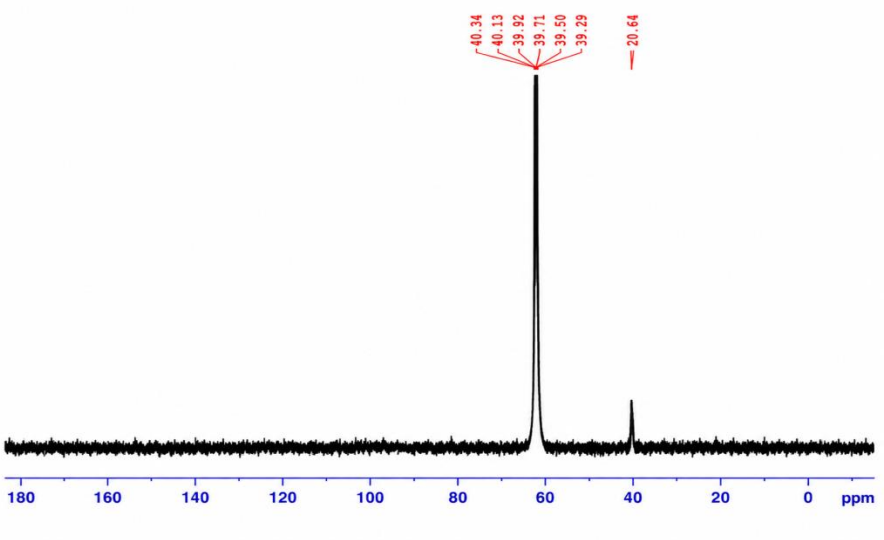

Fig. 2. ^{13}C NMR spectrum of the synthesized cellulose acetate

Thermal properties of the cellulose acetate. Thermogravimetric analysis (TGA) of the modified cellulose exhibited a multi-step degradation pattern as illustrated in Fig. 3. A slight initial weight loss observed below 100°C is attributed to the evaporation of physically adsorbed moisture and residual volatile compounds, suggesting the relatively low water affinity towards acetylated cellulose. The principal degradation step, occurring roughly between 250 and 380°C, represents a sharp mass decline and is associated with deacetylation owing to thermal cleavage of acetyl groups, resulting in breakdown of the polymer backbone. Above 400°C, a gradual mass loss was observed, which can be ascribed to further degradation and carbonization of the residual char. The minimal remaining mass at 800°C (96.5% total weight loss) reflects the substantial organic content and high purity of the acetylated cellulose with minimal inorganic impurities. These findings align with earlier research published by Caballero [33] and Das et al. [34].

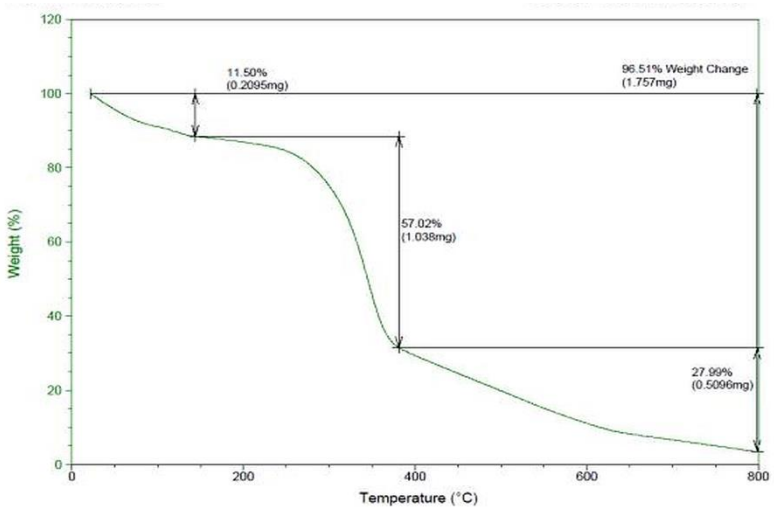

Fig. 3. TGA curve for the cellulose acetate sample

Morphological study of cellulose acetate. The morphological features of the synthesized cellulose acetate sample were evaluated using the SEM technique. The SEM images (Fig. 4) revealed a smooth surface and tightly packed architecture, suggesting an effective acetylation process with minimal impurities. It can be observed that no noticeable defects or pores were found, indicating consistent morphology and excellent film-forming features. At higher magnification, the cellulose fiber structure remains partially intact, reflecting that the acetylation process preserved the native micro-fibrillar architecture while functionalizing the polymer with acetyl groups.

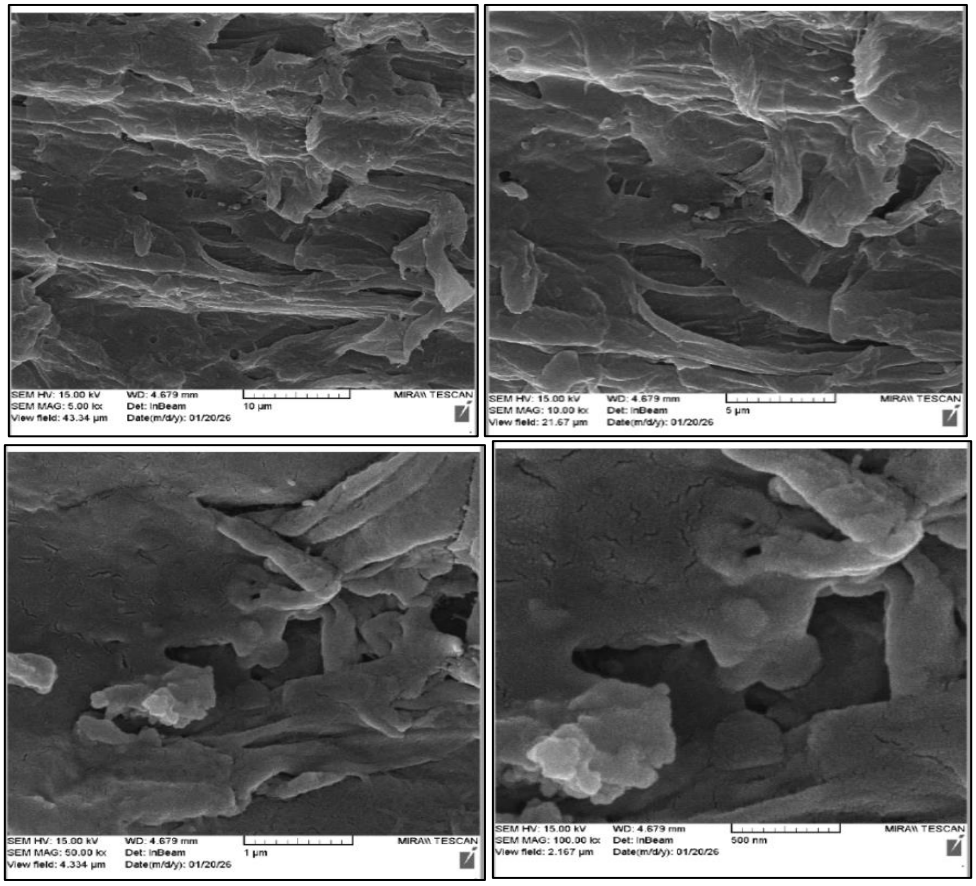

Fig. 4. SEM images of cellulose acetate with magnification 5 kx, 10 kx, 50 kx, 100 kx.

Such morphology is expected to enhance the material's mechanical performance, thermal behavior, and suitability for use in eco-friendly films and membranes. These results agree with

previously published studies on cellulose acetate [35-38], confirming that SEM micrographs commonly reveal a uniform morphology with retained fibrous nature.

X-ray diffraction (XRD) analysis of cellulose acetate. The XRD profile of the synthesized cellulose acetate was recorded in the 2θ range from 10° to 80° using Cu Kα. The diffraction pattern exhibited a dominant broad peak that appeared around 23.2°, accompanied by low intensity peaks centered at 15.1°, 34.6°, and 47.9° (Fig. 5). The prominent broad band reflects the largely amorphous nature of cellulose acetate. The reduction of crystalline peaks relative to native cellulose form indicates disruption of its hydrogen bonding network caused by substituting hydroxyl groups with acetyl groups during the acetylation reaction. The diffraction peak at 23.2° is generally associated with the semi-crystalline region of cellulose acetate, while its broad nature confirms reduced crystallinity and a higher amorphous feature. Overall, these findings verified successful cellulose acetylation, resulting in the diminishing of crystallinity and enhanced amorphous character, in agreement with previous published XRD studies of cellulose acetate [39-41].

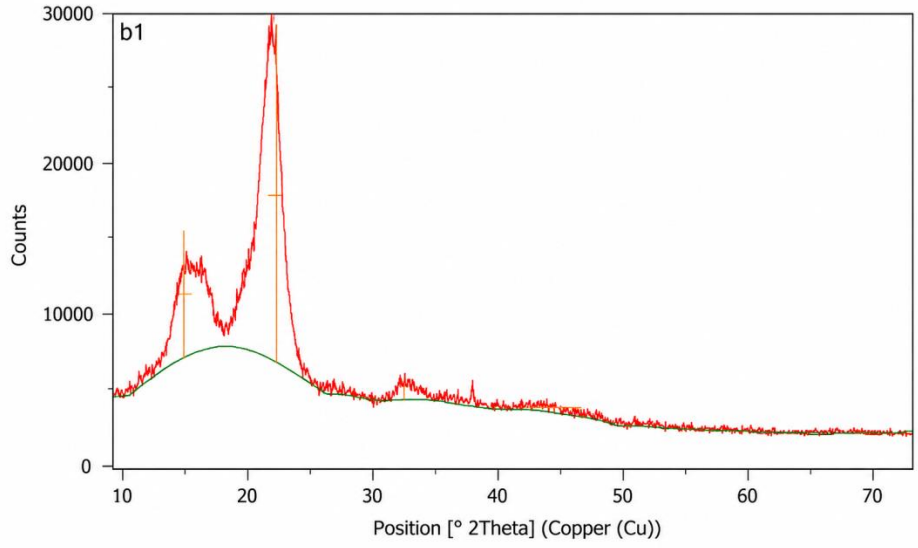

Fig. 5. XRD pattern of the synthesized cellulose acetate

Bioethanol production. Bioethanol production from biomass (cotton stalk) was effectively performed using a series of mechanical, chemical, and biological processes. Mechanical grinding markedly reduced particle size and extended surface area, facilitating cellulose accessibility during chemical treatment. Acid pretreatment at different concentrations effectively disrupted the lignocellulosic framework by removing hemicellulose and partial lignin, which enhanced the accessibility of fermentable fibers. High acid concentrations improved hemicellulose and lignin removal; however, excessive acidity led to the formation of inhibitors, including furfural and hydroxymethyl furfural (HMF) as by-products, which negatively impact the fermentation process and bioethanol production. Whereas low acid levels resulted in incomplete biomass disruption, providing lower sugar release and bioethanol production. Upon completion of acid pretreatment, the washing step using distilled water significantly reduced residual acidity and inhibitory by-products, thereby creating a more suitable environment for yeast (S cerevisiae) activity and fermentation process. The transformation of bioethanol from cotton stalks was enhanced under optimized conditions. Conducting temperature at 32°C supported efficient yeast growth and metabolic performance for the fermentation process. The slightly acidic medium (pH = 4-5) in the fermented solution promoted yeast activity and restricted bacterial interference, leading to higher fermentation performance. Furthermore, fermentation time played a critical role in bioethanol yield. During the initial stage, bioethanol concentration increased progressively owing to rapid sugar conversion, reaching a maximum at the optimal period (48-72 h). In this study, the grounded cotton stalk was subjected to acid pretreatment using phosphoric acid (H_3PO_4) at concentrations of 0.5%, 1.0%, and 1.5% (acid solution to solid cotton stalk ratio of 10:1 mL/mg), then a fermentation process using S.

cerevisiae under anaerobic conditions as listed in Table 1. After fermentation, purification of the obtained bioethanol via suitable separation techniques such as distillation and dehydration, confirmed that acid pretreatment severity affects ethanol yield.

It is noteworthy that the selection of phosphoric acid (H_3PO_4) for biomass hydrolysis offers several advantages compared with conventional mineral acids such as sulfuric acid (H_2SO_4) and hydrochloric acid (HCl). Phosphoric acid is less corrosive, less toxic, and easier to handle, thereby reducing equipment degradation and operational hazards. In addition, it promotes effective disruption of the lignocellulosic structure while limiting the formation of inhibitory degradation products such as furfural and 5-hydroxymethylfurfural (HMF), which can adversely affect subsequent fermentation processes. Furthermore, phosphate-containing hydrolysates may provide nutrients beneficial for microbial growth, enhancing the sustainability of the bioconversion process. These characteristics make phosphoric acid a promising and environmentally favorable alternative for biomass pretreatment and hydrolysis.

Table 1. Experimental data for acid treatment of cotton stalk as feedstock and fermentation conditions

Sample	Concentration of acid (H_3PO_4) at ratio of 10:1 acid to waste (mL/g)	Acid treatment time (hours)	pH value	Bioethanol yield (%)	Fermentation period (Hours)
Sample 1	0.5	3	4.7^b-5.1^a	20.1	72
Sample 2	1.0	3	4.5^b-5.2^a	37.5	72
Sample 3	1.5	3	4.0^b-4.8^a	34.5	72

b - before fermentation process; *a* - after fermentation process

It can be noted that acid concentration influenced bioethanol production. The 0.5% H_3PO_4 treatment yielded 20.1% bioethanol (Sample 1) as illustrated in Fig. 6, suggesting insufficient lignocellulosic disruption and limited sugar release, whereas increasing the concentration to 1.0% enhanced structural breakdown and fermentable sugar release, resulting in the maximum ethanol yield of 37.5% as labeled (Sample 2). These results suggest that a 1.0% acid concentration provides the optimal pretreatment severity, ensuring an appropriate balance between effective disruptions of cellulosic structure and preserving fermentable sugars. However, further increasing the acid concentration to 1.5% decreased ethanol yield (34.5%) as referred to in Sample 3, which is probably due to excessive sugar hydrolysis and inhibitor formation, such as furfural and HMF.

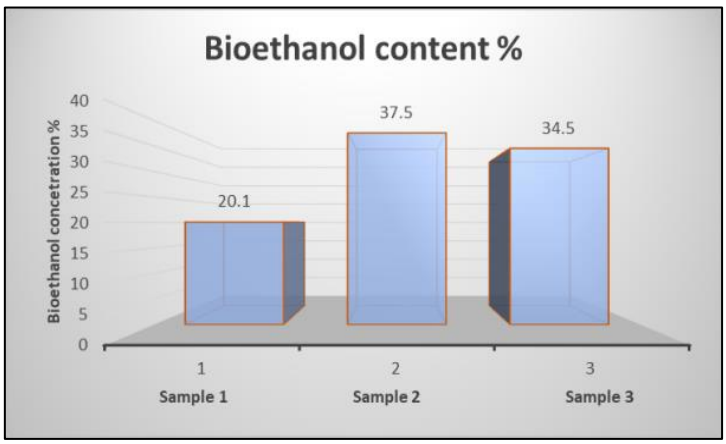

Fig. 6. Bioethanol yields of cotton stalk using different acid pretreatment conditions.

Characterizations of the produced bioethanol. FTIR spectroscopy was employed to verify the functional groups and evaluate the purity of the obtained bioethanol samples at different acid pretreatment conditions. The FTIR spectra of all samples, as shown in Fig.s 7a, b, and c, displayed the typical absorption bands associated with bioethanol structure, indicating a successful

fermentation process. It can be observed that a broad absorption peak approximately at 3300 cm^{-1} corresponds to (-OH) stretching vibrations, confirming the presence of functional hydroxyl groups. The absorption peaks between 2880 and 2980 cm^{-1} reflect aliphatic C-H stretching bonds in CH_2 and CH_3 groups. Furthermore, other sharp peaks around 1045-1087 cm^{-1} represent C-O stretching, verifying a key fingerprint of ethanol. In summary, the FTIR analysis verified successful bioethanol production regardless of acid pretreatment severity. The FTIR findings of the current investigation are consistent with previously published reports [1, 2, 9, 42].

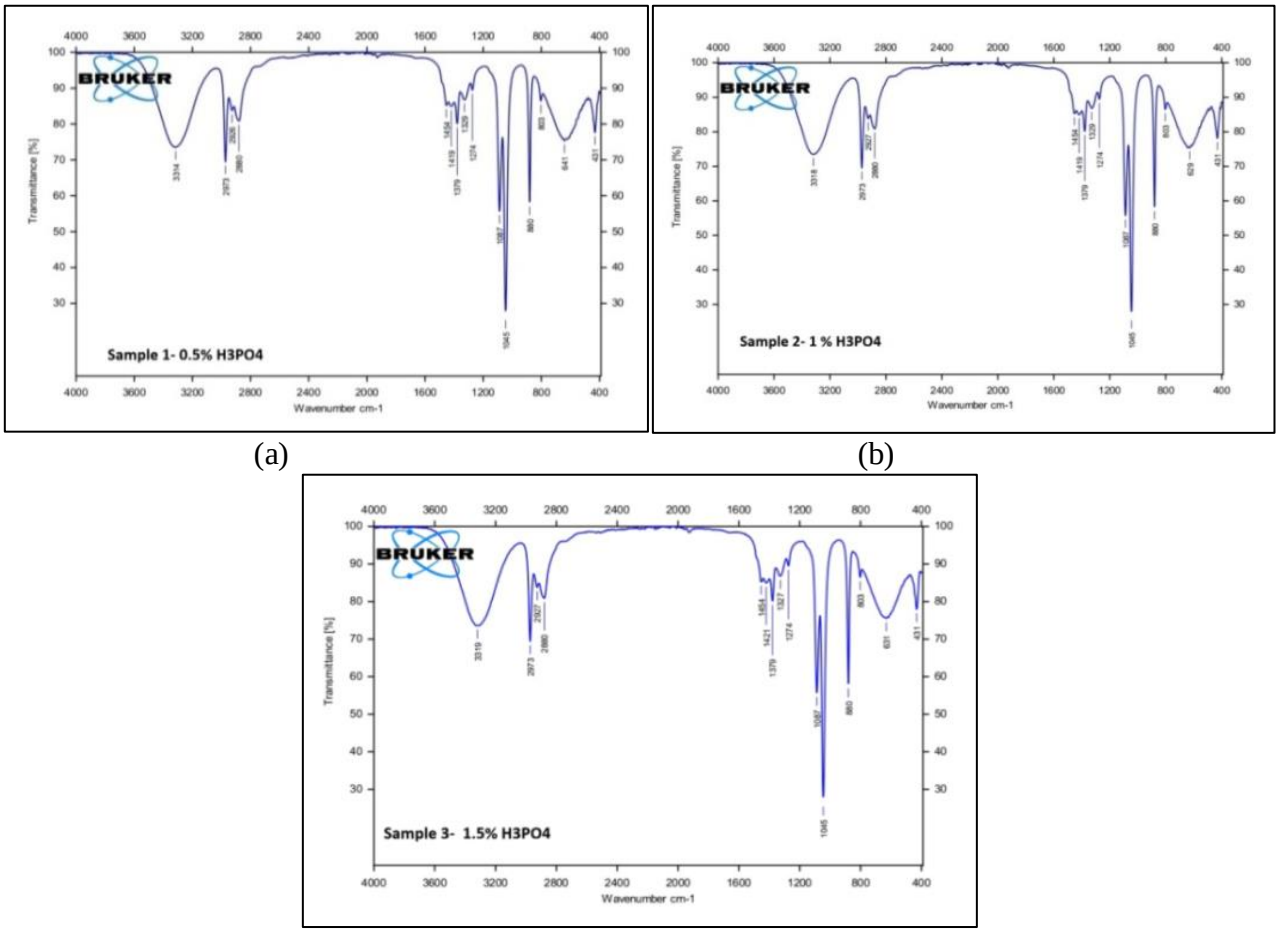

Fig. 7. FTIR spectra of the obtained bioethanol from sample 1 at 0.5% H_3PO_4 pretreatment (a), sample 2 at 1.0% H_3PO_4 pretreatment (b), sample 3 at 1.5% H_3PO_4 pretreatment (c)

The bioethanol sample, which was collected from a different fermentation process, was analyzed using the ^{1}H-NMR technique to confirm chemical identity and purity. The ^{1}H-NMR spectra (Fig. 8) exhibited the typical ethanol resonance, including a triplet peak at 0.78-1.13 ppm assigned to the methyl (-CH_3) group and a quartet peak around 3.20-3.81 ppm corresponding to the methylene (-CH_2-) group next to the oxygen atom. Moreover, a singlet peak appearing at 4.63 ppm was attributed to the OH proton. It can also be noticed that the 3:2 integration ratio between the methyl and methylene peaks further confirmed the ethanol formation as a main product. The spectroscopic findings are in good agreement with ethanol yield data, and previous published works by [2, 43, 44], verifying successful ethanol production and purity.

The recorded ^{13}C-NMR results confirmed the successful formation and purity of bioethanol via the fermentation process. As shown in Fig. 9, it can be observed that two prominent carbon signals were detected at approximately 17.5 ppm for the methyl group (-CH_3) and another peak around 57.0 ppm corresponding to the methylene group (-CH_2-) attached to oxygen. Furthermore, the deuterated chloroform $CDCl_3$ peak appeared near 76.8-77.5 ppm. The absence of additional peaks reflects the high chemical purity of bioethanol.

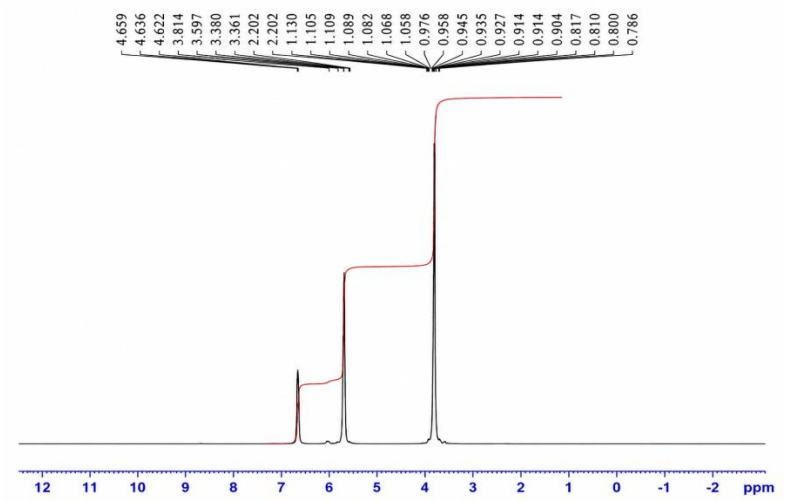

Fig. 8. ^{1}H-NMR spectrum of the obtained bioethanol

The obtained data are consistent with previously published studies [9, 45, 46] that validated bioethanol structure and purity using the ^{13}C-NMR technique.

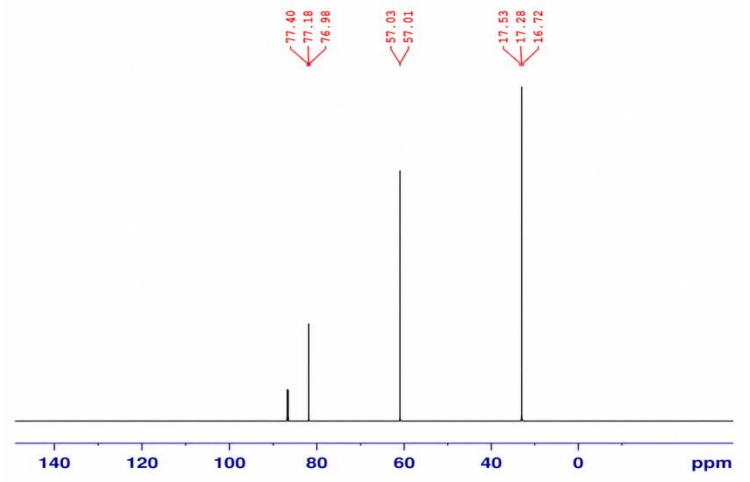

Fig. 9. ^{1}H NMR spectrum of the obtained bioethanol.

Bioethanol-gasoline blends. This current work further investigated the performance of bioethanol-gasoline blended fuel at different bioethanol ratios to determine their potential application as an alternative fuel for internal combustion engines. Fuel characteristics, including density, RVP, RON, and water content, were evaluated according to ASTM standard procedures as listed in Table 2.

Table 2. Physiochemical characteristics of pure gasoline and binary fuel mixtures at various blending ratios

Properties	ASTM standard test	Bioethanol ratio in the fuel			
		E0 (0%)	E5 (5%)	E7 (7%)	E10 (10%)
Density (g/cm^3 at 15.5 °C)	*ASTM-D4052*	0.7220	0.7290	0.7344	0.7371
RVP (Kpa at 37 °C)	*ASTM-D6378*	70.0	66.2	64.9	63.1
RON	*ASTM-D2699*	82.0	85.0	87.0	89.0
Water content (ppm)	*ASTM- D6304*	35	1340	1710	2110
Color	yellow	yellow	yellow	yellow	yellow

Overall, the density of base gasoline (E0) was found to be lower relative to that of binary fuel mixtures containing 5% (E5), 7% (E7), and 10% (E10) bioethanol. A modest increase in density was observed with increasing bioethanol ratios (0%, 5%, 7%, and 10%), as shown in Fig. 10. The behavior can be attributed to the higher specific density of bioethanol (0.789 g/cm^3) relative to pure gasoline (0.72-0.75 g/cm^3). Hence, higher bioethanol fractions in binary mixtures contribute to a gradual increase in the fuel mixtures. Furthermore, the density values meet ASTM standards, suggesting that E5-E10 binary mixtures are suitable for standard gasoline engines without significant modifications to the existing fuel system. Similar observations were reported in a previous study by Bassiouny et. al. [47], showing that blending ethanol with gasoline at various ratios (E5, E10, E15, and E20) increased the density compared to untreated gasoline (E0).

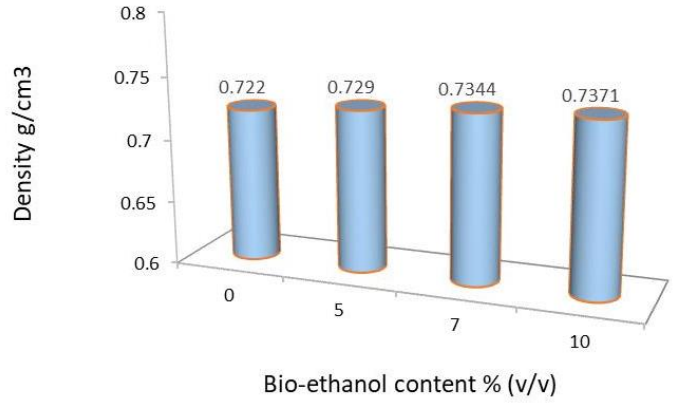

Fig. 10. Relationship between the density and bioethanol volumetric percentage in bioethanol-gasoline blends (E0, E5, E7, and E10)

The RVP value of untreated gasoline (E0) was observed to be higher than that of bioethanol-gasoline-blended fuels (E5, E7, and E10) as depicted in Fig. 11. A remarkable decline in RVP value was noted as the bioethanol fraction increased from 5% to 10%, reflecting a gradual reduction in fuel volatility with increasing bioethanol content. This observed decline can be attributed to the low vapor pressure of bioethanol in contrast to highly volatile gasoline components [48]. The RVP values of binary mixtures are moderate and suitable for internal combustion engines as summer-grade fuel. In summary, the obtained RVP values fall within standard fuel specifications, making these binary mixtures (E5, E7, and E10) also appropriate for summer-grade fuel operation.

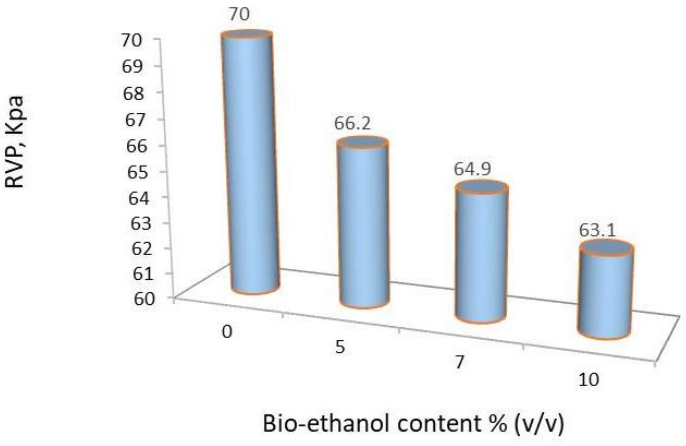

Fig. 11. Relationship between the RVP and bioethanol volumetric percentage in bioethanol-gasoline blends (E0, E5, E7, and E10)

The untreated gasoline (E0) exhibited a lower RON value of 82 than its corresponding bioethanol blends (E5, E7, and E10) at 84, 87, and 89, respectively (Fig. 12). As the bioethanol

content increased from 5% to 10%, an improvement in octane rating was noted, confirming improved anti-knock features upon bioethanol incorporation. It can be concluded that there is a direct relation between bioethanol ratio and octane enhancement. This behavior can be ascribed to the high octane rating of bioethanol (approximately 108-109) [49], which is greater than that of conventional gasoline. Furthermore, the oxygenated nature of ethanol promotes the combustion properties of fuel and is cleaner. These RON values of bioethanol-gasoline blends are consistent with fuel specifications established by ASTM-D2699, which evaluates the anti-knocking performance of pure gasoline and gasoline-oxygenate blends. The current data are consistent with earlier studies on the effect of blended feedstocks on gasoline octane number. Ultimately, controlled bioethanol addition enhances the anti-knock characteristics of spark ignition fuels.

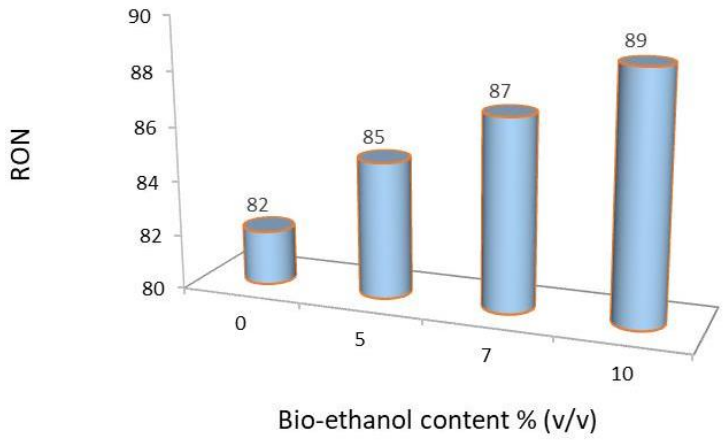

Fig. 12. Relationship between the RON and bioethanol volumetric percentage in bioethanol-gasoline blends (E0, E5, E7, and E10)

The water content of pure gasoline (35 ppm) (Fig. 13) was significantly lower than that of binary mixtures, where water content values increased to reach 1340 ppm, 1710 ppm, and 2110 ppm for E5, E7, and E10, respectively. This trend highlighted that higher bioethanol ratios result in larger water retention in the fuel blends. This trend can be attributed to the hygroscopic nature of alcohol. The presence of the polar hydroxyl –OH would enhance the hydrogen bonding with water, resulting in high affinity and moisture absorption during blending and in the storage environment However, water content around 1500-200 ppm may promote phase separation in the binary mixtures, especially under low-temperature conditions [50, 51].

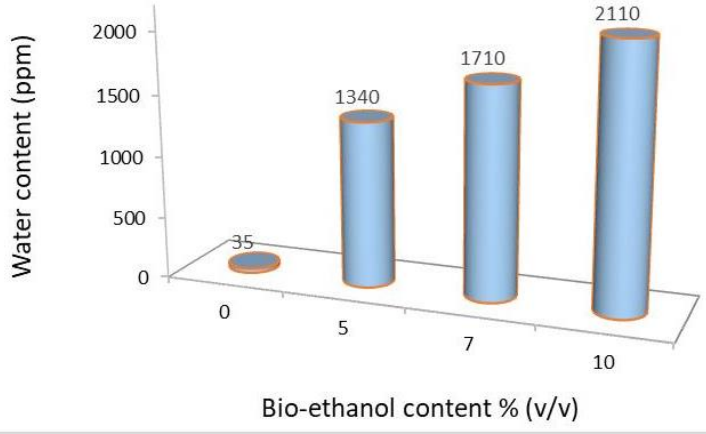

Fig. 13. Relationship between the water content and bioethanol volumetric percentage in bioethanol-gasoline blends (E0, E5, E7, and E10)

Conclusion

This current work indicated that cotton stalks can be efficiently converted and used as a promising sustainable feedstock for producing high-value polymers and biofuels. Initially, cellulose was successfully extracted from cotton stalk and then acetylated to form cellulose acetate, suggesting the capability of transforming lignocellulosic waste into an advanced biopolymer. The synthesized polymer was structurally confirmed using ^{1}H and ^{13}C NMR spectroscopy and CHNS, indicating the successful acetyl group incorporation. Molecular weight characterization using the GPC technique indicated a relatively moderate molecular weight, suggesting an effective acetylation process, while SEM profiles exhibited a uniform and homogenous acetylated surface of cellulose acetate. In the second stage, the cotton stalk was subjected to dilute acid pretreatment using different concentrations (0.5%, 1.0%, and 1.5%) of H_3PO_4 to release fermentable. Following fermentation and purification processes, bioethanol yields of 20.1%, 37.5%, and 34.5% were obtained, respectively, highlighting 1.0% H_3PO_4 as the most favorable concentration for the conversion process. The structural identity and purity of the obtained bioethanol were verified by the NMR technique, suggesting successful alcoholic fermentation. Finally, the produced bioethanol was blended with normal gasoline at various volumetric ratios to formulate fuel blends. Fuel property analysis exhibited that bioethanol incorporation influenced RON, RVP, density, and moisture content. Notably, the increase in RON indicates the role of bioethanol as an octane enhancer, while the other physiochemical properties were within technically acceptable ranges. It is recommended that future research should focus on determining the critical water content that induces phase separation in bioethanol–gasoline blends containing 5%, 7%, and 10% bioethanol. Such studies are essential for assessing storage stability, fuel quality preservation, and the practical implementation of these blends under different environmental and operational conditions. In summary, this current study highlighted a viable and sustainable approach for transforming biomass into valuable cellulose acetate and renewable fuel products. Such an integrated route contributes sustainable energy utilization within a circular economy system.

Conflict of interest.
The authors announced that there are no conflicts of interest regarding this current work.

Acknowledgment.
We would like to thank the University of Mosul for providing the necessary facilities, laboratory, sophisticated instrument, and technical support to perform this research.

References

1. Al-Abdallha N.G., Al-Azzawi A.G. Optimisation of bioethanol production using cardboard waste as a promising feedstock via the yeast fermentation process. *Bulletin of the Chemical Society of Ethiopia*, 2025, **Vol. 39(8)**, p. 1621-1637. DOI: 10.4314/bcse.v39i8.13
2. Alsaayigh M., Al-Azzawi A. Using waste paper as a promising feedstock for bio-ethanol fuel production with consequence purification using distillation technique and molecular sieve. *Chemical Problems*, 2025, **Vol. 23(1)**, p. 20-35. DOI: 10.32737/2221-8688-2025-1-20-35
3. Prakash S., Radha, Sharma K., Dhumal S., Senapathy M., Deshmukh V.P., Kumar S., Madhu, Anitha T., Balamurugan V. Unlocking the potential of cotton stalk as a renewable source of cellulose: A review on advancements and emerging applications. *International Journal of Biological Macromolecules*, 2024, **Vol. 261,** 129456. DOI: 10.1016/j.ijbiomac.2024.129456
4. Mohammed H.A., Hussein I.I., Hamasalih G.H., Al-Azzawi A.G.S., Mohammed P.A., Al-Saeedi S.I., Aziz Sh.B., Hassan J. Investigation of structural and optoelectronic properties in dye-doped MC biopolymer films. *Journal of Science: Advanced Materials and Devices*, 2025, **Vol. 10(4)**, 100968. DOI: 10.1016/j.jsamd.2025.100968

5. Ghazal R.Y., Al-Azzawi A.G., Ali M.H. Zeolite formation using structural directing agent to enhance heavy naphtha via reforming processes. *Chemical Problems*, 2025, **Vol. 23(2)**, p. 187-201. DOI: 10.32737/2221-8688-2025-2-187-201
6. Subramanian K., Sarkar M.K., Wang H., Qin Z.H., Chopra S.S., Jin M., Kumar V., Chen Ch., Tsang Ch.-W., Lin C.S.K. An overview of cotton and polyester, and their blended waste textile valorisation to value-added products: A circular economy approach–research trends, opportunities and challenges. *Critical Reviews in Environmental Science and Technology*, 2022, **Vol. 52(21)**, p. 3921-3942. DOI: 10.1080/10643389.2021.1966254
7. Shaghaleh H., Xu X., Wang S. Current progress in production of biopolymeric materials based on cellulose, cellulose nanofibers, and cellulose derivatives. *RSC advances*, 2018, **Vol. 8(2)**, p. 825-842. DOI: 10.1039/C7RA11157F
8. Bhaladhare S., Das D. Cellulose: A fascinating biopolymer for hydrogel synthesis. *Journal of Materials Chemistry B*, 2022, **Vol. 10(12)**, p. 1923-1945. DOI: 10.1039/D1TB02848K
9. Saleh S., Ahmed A.-A. Optimizing Bioethanol Production for High Octane Bioethanol-Gasoline Blended Fuel through Fermentation. *Journal of the Turkish Chemical Society Section A: Chemistry*, 2023, **Vol. 10(2)**, p. 475-486. DOI: 10.18596/jotcsa.1250955
10. Al-Azzawi A.G., Iraqi A., Sadoon A.M., Esmaeel O.M., Karomi I.B. Experimental and theoretical study of linker effects on electrochemical and optical properties of alternating conjugated polymers. *Chemical Data Collections*, 2025, **Vol. 60**, 101208. DOI: 10.1016/j.cdc.2025.101208
11. An Y., Li F., Di Y., Zhang X., Lu J., Wang L., Yan Zh., Wang W., Liu M., Fei P. Hydrophobic modification of cellulose acetate and its application in the field of water treatment: a review. *Molecules*, 2024, **Vol. 29(21)**, 5127. DOI: 10.3390/molecules29215127
12. Rajeswari A., Jackcina Stobel Christy E., Swathi E., Pius A. Fabrication of improved cellulose acetate-based biodegradable films for food packaging applications. *Environmental Chemistry and Ecotoxicology*, 2020, **Vol. 2,** p. 107-114. DOI: 10.1016/j.enceco.2020.07.003
13. Bello A., Isa M.T., Aderemi B.O., Mukhtar B. Acetylation of cotton stalk for cellulose acetate production. *American Scientific Research Journal for Engineering, Technology, and Sciences*, 2016, **Vol. 15(1)**, p. 137-150.
14. Al-Azzawi A.G. Investigation of rheological properties of asphalt mixtures containing polymer waste. *Egyptian Journal of Chemistry*, 2022, **Vol. 65(6)**, p. 327 - 337. DOI: 10.21608/EJCHEM.2021.103100.4777.
15. Blasi A., Verardi A., Lopresto C.G., Siciliano S., Sangiorgio P. Lignocellulosic agricultural waste valorization to obtain valuable products: An overview. *Recycling*, 2023, **Vol. 8(4)**, 61. DOI: 10.3390/recycling8040061
16. Mamand D.M., Aziz D.M., Khasraw S.S., Al-Azzawi A.G.S., Al-Saeedi S.I., Aziz Sh.B., Hassan J. Improved optical characteristics of PEO polymer integrated with graphene oxide. *Scientific Reports*, 2025, **Vol. 15(1)**, 32225. DOI: 10.1038/s41598-025-16778-9
17. Esmaeel O.M., Iraqi A., Al-Azzawi A.G.S., Karomi I.B., Shareef B.A. Synthesis and characterization of two novel pyrene-based conjugated polymers: optical, electrochemical, morphological, and thermal properties. *Optical Materials*, 2025, **Vol. 160**, 116693. DOI: 10.1016/j.optmat.2025.116693
18. Wang M., Zhou D., Wang Y., Wei Sh., Weihua Y., Kuang M., Ma L., Fang D., Xu Sh., Du Sh.-k. Bioethanol production from cotton stalk: a comparative study of various pretreatments. *Fuel*, 2016, **Vol. 184,** p. 527-532. DOI: 10.1016/j.fuel.2016.07.061
19. Bano A., Irfan M. Alkali pretreatment of cotton stalk for bioethanol. *Bangladesh Journal of Scientific and Industrial Research*, 2019, **Vol. 54(1)**, p. 73-82. DOI: 10.3329/bjsir.v54i1.40733
20. Malik K., Salama E.-S., El-Dalatony M.M., Jalalah M., Harraz F.A., Al-Assiri M.S., Zheng Y., Sharma P., Li X. Co-fermentation of immobilized yeasts boosted bioethanol production from pretreated cotton stalk lignocellulosic biomass: Long-term investigation. *Industrial Crops and Products*, 2021, **Vol. 159,** 113122. DOI: 10.1016/j.indcrop.2020.113122

21. Dey S., Banerjee S., Banerjee R. Biotransformation of cotton stalk to bioethanol by an environmentally benign enzymatic route. *Biomass and Bioenergy*, 2026, Vol. **208,** 108802. DOI; 10.1016/j.biombioe.2025.108802
22. Silverstein R.A., Chen Y., Sharma-Shivappa R.R., Boyette M.D., Osborne J. A comparison of chemical pretreatment methods for improving saccharification of cotton stalks. *Bioresource technology*, 2007, **Vol. 98(16)**, p. 3000-3011. DOI: 10.1016/j.biortech.2006.10.022
23. Heinze T., Liebert T. Unconventional methods in cellulose functionalization. *Progress In Polymer Science*, 2001, **Vol. 26(9)**, p. 1689-1762. DOI: 10.1016/S0079-6700(01)00022-3
24. Edgar K.J., Buchanan Ch.M., Debenham J.S., Rundquist P.A., Seiler B.D., Shelton M.C., Tindall D. Advances in cellulose ester performance and application. *Progress In Polymer Science*, 2001, **Vol. 26(9)**, p. 1605-1688. DOI: 10.1016/S0079-6700(01)00027-2
25. Andrade J., Prada D., Muniategui S. Manual or automatic methods for gravity determinations in heavy petroleum distillates? Structured evaluation of automation. *Laboratory Automation & Information Management*, 1995, **Vol. 31(2)**, p. 89-98. DOI: 10.1016/1381-141X(95)80025-X
26. Mozaffari P., Baird Z.S., Listak M., Oja V. Vapor pressures of narrow gasoline fractions of oil from industrial retorting of Kukersite oil shale. *Oil Shale*, 2020, **Vol. 37(4)**, p. 288-303. DOI: 10.3176/oil.2020.4.03
27. Kolodziej C.P., Wallner T. Combustion characteristics of various fuels during research octane number testing on an instrumented CFR F1/F2 engine. *Combustion Engines*, 2017, **Vol. 56(4)**, p. 164-169. DOI: 10.19206/CE-2017-427
28. Lin M.-J., Research the Instrument of Karl Fischer Titration How to Detect the Moisture Content from Transformer Insulating Oil. *Journal of Engineering Research and Reports*, 2023, **Vol. 24(8)**, p. 46-51. DOI: 10.9734/jerr/2023/v24i8837
29. Calvin Y.L., Hariyanto P.A.T., Usman A.I., Masuku M., Wibowo C.S., Maymuchar, Anggarani R., Fathurrahman N.A., Sugiarto B. Volatility and physicochemical properties of gasoline-ethanol blends with gasoline RON-based 88, 90, and 92. *Fuel*, 2022, **Vol. 307**, 121850. DOI: 10.1016/j.fuel.2021.121850
30. Klemm D., Heublein B., Fink H.-P., Bohn A. Cellulose: fascinating biopolymer and sustainable raw material. *Angewandte Chemie International Edition*, 2005, **Vol. 44(22)**, p. 3358-3393. DOI: 10.1002/anie.200460587
31. Kono H., Oka Ch., Kishimoto R., Fujita S. NMR characterization of cellulose acetate: mole fraction of monomers in cellulose acetate determined from carbonyl carbon resonances. *Carbohydrate Polymers*, 2017, **Vol. 170,** p. 23-32. DOI: 10.1016/j.carbpol.2017.04.061
32. Hu H., Li H., Zhang Y., Chen Y., Huang Z., Huang A., Zhu Y., Qin X., Lin B. Green mechanical activation-assisted solid phase synthesis of cellulose esters using a co-reactant: effect of chain length of fatty acids on reaction efficiency and structure properties of products. *RSC advances*, 2015, **Vol. 5(27)**, p. 20656-20662. DOI: 10.1039/C5RA02393A
33. Caballero J.A., Conesa J.A. Mathematical considerations for nonisothermal kinetics in thermal decomposition. *Journal Of Analytical And Applied Pyrolysis*, 2005, **Vol. 73(1)**, p. 85-100. DOI: 10.1016/j.jaap.2004.12.003
34. Das D., Maiti S., Maiti T.K., Islam S.S. A new arabinoxylan from green leaves of Litsea glutinosa (Lauraeae): structural and biological studies. *Carbohydrate Polymers*, 2013, **Vol. 92(2)**, p. 1243-1248. DOI: 10.1016/j.carbpol.2012.10.052
35. Wu S., Qin X., Li M. The structure and properties of cellulose acetate materials: A comparative study on electrospun membranes and casted films. *Journal of Industrial Textiles*, 2014, **Vol. 44(1)**, p. 85-98. DOI: 10.1177/1528083713477443
36. Maryudi M., Hakika D.C., Amillia A. Morphology and selected properties of cellulose acetate membranes for environmental applications. *Polimery*, 2024, **Vol. 69(5)**, p. 292-299. DOI: 10.14314/polimery.2024.5.2
37. Al-Azzawi A.G., Ghazal R.Y. Evaluation of Rheological and Thermal Behavior of Polymer Modified Asphalt. *Egyptian Journal of Chemistry*, 2022, **Vol. 65(11)**, p. 1-10. DOI; 10.21608/ejchem.2022.121228.5446

38. Al-Azzawi A., Hamdoon A. Mechanical performance study of asphalt by waste plastics and waste engine oil. *AIP Conference Proceedings*, 2020, **Vol. 2213**, 020158. DOI: 10.1063/5.0000199
39. Ezzat D., Youssif M., Elhaes H., El-Nahass M. XRD and UV–Vis studies of cellulose acetate film blended with different concentrations of nano-metal oxide. *Optical and Quantum Electronics*, 2024, **Vol. 56(5)**, 839. DOI: 10.1007/s11082-024-06480-x
40. Mbacke M.K., Ndoye M., Sene M. Nanofiltration membranes based on cellulose triacetate from millet husk. *RSC Sustainability*, 2026, **Vol.4(3)**, p. 1464-1484. DOI: 10.1039/d5su00889a
41. Al-Azzawi A.G., Dannoun E.M.A., Aziz S.B., Iraqi A., Al-Saeedi S.I., Nofal M.M., Murad A.R. Synthesis and Characterization of Polymers Containing Ethynylene and Ethynylene-Thiophene Based Alternating Polymers Containing 2, 1, 3-Linked Naphthothiadiazole Units as Acceptor Linked with Fluorine as Donor: Electrochemical and Spectroscopic Studies. *Polymers*, 2022, **Vol. 14(19)**, 4139. DOI: 10.3390/polym14194139
42. Hamden Z., El-Ghoul Y., Alminderej F.M., Saleh S.M., Majdoub H. High-quality bioethanol and vinegar production from Saudi Arabia dates: Characterization and evaluation of their value and antioxidant efficiency. *Antioxidants*, 2022, **Vol. 11(6)**, 1155. DOI: 10.3390/antiox11061155
43. Shi J., Lu X., Yu R., Zhu W. Nutrient removal and phosphorus recovery performances of a novel anaerobic-anoxic/nitrifying/induced crystallization process. *Bioresource Technology*, 2012, **Vol. 121**, p. 183-189. DOI: 10.1016/j.biortech.2012.06.064
44. Zabed H., Sahu J.N., Suely A., Boyce A.N., Faruq G. Bioethanol production from renewable sources: Current perspectives and technological progress. *Renewable and Sustainable Energy Reviews*, 2017, **Vol. 71,** p. 475-501. DOI: 10.1016/j.rser.2016.12.076
45. Gilbert A., Hattori R., Silvestre V., Wasano N., Akoka S., Hirano S., Yamada K., Yoshida N., Remaud G.S. Comparison of IRMS and NMR spectrometry for the determination of intramolecular 13C isotope composition: Application to ethanol. *Talanta*, 2012, **Vol. 99,** p. 1035-1039. DOI: 10.1016/j.talanta.2012.05.023
46. Chamberlain P.H. Identification of an Alcohol with 13C NMR Spectroscopy. *Journal of Chemical Education*, 2013, **Vol. 90(10)**, p. 1365-1367. DOI: 10.1021/ed300833s
47. El-Bassiouny A., Aboul-Fotouh T.M., Abdellatief T.M. Maximize the production of environmental, clean and high octane number gasoline-ethanol blends by using refinery products. *Int. J. Sci. Eng. Res*, 2015, **Vol. 6(7)**, p. 1792-1803.
48. Murachman B., Pranantyo D., Putra E.S. Study of gasohol as alternative fuel for gasoline substitution: characteristics and performances. *International Journal of Renewable Energy Development*, 2014, **Vol. 3(3)**, 175. DOI: 10.14710/ijred.3.3.175-183
49. Sindhu R., Binod P., Pandey A., Ankaram S., Duan Y., Awasthi M.K. *Biofuel production from biomass: toward sustainable development, in Current developments in biotechnology and bioengineering*. Chapter 5 - Biofuel Production From Biomass: Toward Sustainable Development. Elsevier. 2019. p. 79-92. DOI; 10.1016/B978-0-444-64083-3.00005-1
50. Shirazi S.A., Abdollahipoor B., Martinson J., Reardon K.F., Windom B.C. Physiochemical property characterization of hydrous and anhydrous ethanol blended gasoline. *Industrial & Engineering Chemistry Research*, 2018, **Vol. 57(32)**, p. 11239-11245. DOI: 10.1021/acs.iecr.8b01711
51. Johansen T., Schramm J. Low-temperature miscibility of ethanol-gasoline-water blends in flex fuel applications. *Energy Sources, Part A*, 2009, **Vol. 31(18)**, p. 1634-1645. DOI: 10.1080/15567030903021897